Diminished gap junction coupling under diabetogenic conditions does not drive loss of functional β-cell sub-populations

Claire H Levitt[a], Dominic Isaacs[a], Maria Hansen[b], Vira Kravets[a], Jennifer K Briggs[a], Richard KP Benninger[a,b,1]

[a] Department of Bioengineering, University of Colorado, Anschutz Medical campus, Aurora, CO. USA

[b] Barbara Davis center for childhood diabetes, University of Colorado, Anschutz Medical campus, Aurora, CO. USA

[1] To whom correspondence should be addressed: richard.benninger@cuanschutz.edu
1775 Aurora court, M20-4306D, mailstop B140, University of Colorado Anschutz Medical campus, Aurora, CO. 80045.

Running Title: Effect of gap junction coupling under diabetogenic conditions

Key Words: Optogenetics, Islet Dynamics; Optical Microscopy; Diabetes; Gap junctions

Classification: Systems Biology

Manuscript word count: 5560
Abstract word count: 282
Number of figures: 5

Abstract

Within the islets of Langerhans, gap junction coupling is important for synchronizing oscillatory free-calcium activity ([Ca^{2+}]) and regulating pulsatile insulin release. In islets from multiple models of diabetes, gap junction coupling is disrupted, and [Ca^{2+}] synchronization and pulsatile insulin is lost. Functional sub-populations have been identified within the islet that are linked to driving synchronized [Ca^{2+}] and insulin release. These sub-populations can be disrupted under conditions associated with diabetes such as glucolipotoxicity and inflammatory environments, and their loss may drive islet dysfunction. Here we investigated how loss of gap junction coupling influences functional subpopulations under diabetogenic environments. We treated islets with a cocktail of pro-inflammatory cytokines, and protected gap junction coupling via co-treatment with a Cx36 peptide S293 that was previously shown to specifically prevent a decline in gap junction permeability and synchronized [Ca^{2+}] dynamics. We performed calcium imaging and ChR2 stimulation, analyzed islet [Ca^{2+}] dynamics and the presence of functional sub-populations including hubs and first-responders. 1h or 24h cytokine-treatment disrupted gap junction coupling, which was fully prevented by S293 peptide co-treatment. Treatment with pro-inflammatory cytokines decreased the recruitment of [Ca^{2+}] upon ChR2 stimulation, increased the time between first and last responding cells upon glucose stimulation, and reduced the number and consistency of hub cells. When preserving gap junction coupling by S293 during cytokine treatment, the presence and consistency of these sub-populations was only marginally improved. We therefore concluded that while gap junction coupling is important for functional sub-populations to exert their influence on islet function, restoration of gap junctions alone is not sufficient to recover functional sub-populations upon diabetogenic conditions. Thus, preventing a disruption to intrinsic β-cell properties that define functional subpopulations is likely important for preserving these sub-populations during diabetes.

Introduction

Diabetes Mellitus (DM) affects approximately 537 million people globally [1,2], and is characterized by the dysfunction and/or death of insulin-secreting β-cells in the islets of Langerhans in the pancreas. β-cells in the islet secrete insulin in response to elevations in blood glucose or other nutrients. At elevated glucose, β-cells show increased ATP/ADP following the metabolism of glucose, which drives membrane depolarization via closure of ATP-sensitive K+ (K_{ATP}) channels and activation of voltage gated calcium (Ca_V) channels. Subsequent oscillations of intracellular free-calcium ([Ca^{2+}]) across the islet drive the release of insulin in discrete pulses.

The dynamics of [Ca^{2+}] are synchronized across β-cells in the islet, which is facilitated by connexin-36 (Cx36) gap junctions [3-5]. Gap junctions synchronize the β-cell response to glucose despite heterogeneity in β-cell metabolism and excitability [6,7]. Under low glucose conditions, gap junction-mediated hyper-polarizing currents suppress spontaneous elevations in [Ca^{2+}] from excitable β-cells [8,9]. At high glucose, gap junction-mediated depolarizing currents coordinate and enhance both first-phase [Ca^{2+}] and oscillatory second phase [Ca^{2+}] responses [3]. In Cx36 knockout models, synchronous [Ca^{2+}] responses are disrupted [3,5,9], both first phase insulin secretion and second phase insulin pulses are diminished and glucose tolerance is impaired [5,10]. Importantly, islet gap junction coupling is disrupted under conditions associated with diabetes including by glucolipotoxicity [2,11,12] and pro-inflammatory cytokines [13] as well as in mouse models of diabetes [14-16] and human [11,12,17]. Synchronous [Ca^{2+}] activity is also disrupted under conditions associated with diabetes [11,13,17,18], likely as a result of disrupted Cx36 gap junction coupling.

β-cells are heterogeneous in gene expression [19-21], glucose sensitivity [6,19], insulin secretion [22], and cell-to-cell communication [23]. As a result, β-cells exhibit functional heterogeneity, and display distinct insulin secretory patterns. This functional heterogeneity is evidenced in previous studies that found ~75% of β-cells exhibited a fixed response to glucose, whereas ~25% fluctuated between states of responsive and unresponsiveness [24]. The characterization of β-cell heterogeneity has led to the identification of functional subpopulations which have been shown to play distinct roles in governing the spatiotemporal [Ca^{2+}] and insulin secretory dynamics of the islet [25,26]. For example, following optogenetic Channelrhodopsin-2 (ChR2) stimulation, a population of β-cells can recruit and elevate [Ca^{2+}] in a large number of neighboring β-cells within the islet [27]. Similarly, 'first-responder cells', that are first to show elevated [Ca^{2+}] upon elevated glucose stimulation, can recruit and coordinate less excitable

cells to respond earlier [28]. This first-responder subpopulation is distinct from previously identified highly-connected 'hub cells' that exhibit a high degree of co-activity with neighboring β-cells [29] and have been shown to play a critical role in driving the synchronized oscillatory dynamics. Importantly, upon both glucolipotoxic environments and pro-inflammatory cytokines, the proportion of 'hub cells' declines [29]. This finding suggests that a selective loss of functional sub-populations may be sufficient to drive islet dysfunction in diabetes. However, the mechanisms underlying this loss of cells are unclear.

In this study, we sought to understand how functional sub-populations of cells are disrupted under conditions associated with diabetes. Given that gap junction coupling influences overall islet coordination, we specifically asked whether the loss of gap junction coupling that is associated with diabetes is a primary cause for the loss of these sub-populations and their influence on islet function. We first tested how functional sub-populations are influenced by pro-inflammatory cytokine treatment. We then tested a role of gap junction coupling, by using a Cx36 peptide [12] that was previously shown to specifically protect gap junction permeability and retain glucose-stimulated [Ca^{2+}] dynamics under conditions associated with diabetes.

101 ***Materials and Methods***

102 *Mice/Animal Care:* Islets expressing ChR2-YFP in β-cells were obtained by crossing Pdx^{PB}-
103 Cre (JAX #014647) and ROSA26-lox-STOP-lox-ChR2-YFP mice (JAX #024109). Islets
104 expressing GCaMP6s in β-cells were obtained by crossing MIP-Cre^{ER} mice (JAX #024709) and
105 ROSA26-lox-STOP-lox-GCaMP6s mice (JAX #028866). Mice were genotyped via qPCR
106 (Transnetyx). All animal experiments were approved by the University of Colorado Institutional
107 Animal Care and Use Committee (IACUC Protocol number: 000024). Mice were housed in a
108 temperature-controlled environment with a 12 hr light/dark cycle and continuous access to both
109 food and water. For mice with β-cell specific GCaMP6s expression, tamoxifen (solubilized in
110 corn oil) was administered via IP injection for 5 consecutive days (50 mg/kg of body weight) to
111 facilitate CreER-mediated recombination. All experiments use both male and female mice.
112

113 *Islet Isolation and Culture:* Islets were isolated from mice under ketamine/xylazine anesthesia
114 and euthanized via exsanguination. Collagenase (Type V, Sigma) was delivered to the
115 pancreases at a concentration of 2.5 mg/mL via the bile duct. After inflation, the pancreas was
116 surgically removed and digested (5 min at 37 °C). Islets were then hand-picked and cultured in
117 RPMI medium (Gibco) containing 10% fetal bovine serum, 100 U/mL penicillin, 100 ug/mL
118 streptomycin, and 11 mM glucose. Islets were incubated at 37°C, 5% CO2.
119

120 *Islet Treatment:* Islets were treated overnight with a cocktail of proinflammatory cytokines (1
121 ng/mL TNF-α, 5 ng/mL IL-1β, and 10 ng/mL IFN-γ), which is equivalent to a '0.1x' cocktail as
122 previously used [13]. To protect gap junction coupling, islets were co-treated with 30 μM
123 peptide S293 for 1-6 hours for experiments using optogenetic stimulation, and 24 hours for
124 experiments measuring gap junction permeability (FRAP) and calcium activity ([Ca^{2+}]).
125

126 *Fluorescent Recovery After Photobleaching and Analysis* Gap junction permeability was
127 assessed by Fluorescence Recovery After Photobleaching (FRAP) [4]. Isolated islets were
128 immobilized onto glass bottom dishes (MatTek) using cell tissue adhesive (CellTak, Corning)
129 and incubated at 37°C, 5% CO2 overnight. Islets were then loaded with 12.5 mM cationic dye
130 Rhodamine-123 (Rh123) for 30 minutes at 37°C in Hank's Balanced Salt Solution (HBSS) at
131 5mM glucose. Islets were washed and imaged at room temperature in HBSS using a Zeiss
132 LSM 800 confocal microscope with a x40 1.2NA water immersion objective. Rh123 was excited

133 at 488 nm. Half the islet area was selected using a rectangular ROI and photobleached for 25
134 frames at 40% laser power, achieving ~50% bleaching on average. Images were collected
135 every 5 seconds for 6 to 10 minutes.

136 Image analysis of Rh123 dye diffusion after photobleaching was conducted using
137 MATLAB and Image J. Fluorescent recovery was measured within a region of interest
138 encompassing the entire photobleached area and individual cells. The initial fluorescence
139 intensity was considered the point directly after photobleaching (I_P). Fluorescence recovery
140 was the final fluorescence (I_F) once the diffusion of dye reached a plateau. The recovery was
141 calculated as a percentage, relative to the initial intensity before photobleaching (I_0) as follows:

142 $$\%\ Recovery = 100 * \frac{I_F - I_P}{I_0 - I_P}$$

143 The rate of fluorescent recovery was calculated based on the linearized exponential fluorescent
144 recovery curve of the bleached area over time (I_i) normalized to the total recovery. Calculations
145 were conducted as follows:

148 $$Rate\ of\ recovery = -Ln(1 - \frac{I_i - I_P}{I_0 - I_P})$$

146 While Rhodamine 123 also loads the mitochondria, dependent on mitochondrial membrane
147 potential, this loading does not influence the measurements of gap junction permeability [12].
149

150 *Channelrhodopsin-2 Single Cell Entrainment and Analysis:* ChR2-YFP expressing islets were
151 incubated with pro-inflammatory cytokines, with or without S293 peptide, or S293 peptide alone
152 for 6 hours after isolation in RPMI medium (Gibco) containing 10% fetal bovine serum, 100
153 U/mL penicillin, 100 ug/mL streptomycin, and 11 mM glucose at 37°C, 5% CO2 prior to study.

154 Islets were loaded with 2μM of calcium indicator Rhodamine-2 (Rhod-2) in BMHH
155 imaging solution (125 mM NaCl, 5.7 mM KCl, 2.5 mM CaCl2, 1.2 mM MgCl2, 10 mM HEPES,
156 2 mM glucose, and 0.1% BSA, pH 7.4) for 35 minutes at 37°C. Islets were then washed and
157 imaged on a glass bottom dish (MatTek) in a 5mM glucose imaging solution using a LSM 800
158 confocal microscope kept at 37°C .

159 ChR2-YFP was excited at 488 nm. A rectangular ROI was drawn within the bounds of a
160 single cell to avoid stimulating neighboring cells that express ChR2-YFP. The cell was activated
161 using a photobleaching macro (intensity 5% laser power) for 8 stimulations at a frequency of
162 0.1 Hz. Rhod-2 was simultaneously excited at 560 nm and the corresponding Ca^{2+} response

across the whole islet was measured based on fluorescent intensity of Rhod-2 that was coincident to ChR2 stimulation.

MATLAB was used to analyze ChR2 recruitment data, as previously described [27], as well as entrainment. Islets were selected by hand drawing a region of interest around the islet. Background was identified as regions that did not show any calcium response. Activity was based on the fluorescent intensity of the Ca^{2+} indicator Rhod-2 upon ChR2 stimulation and assessed using individual pixel time-courses. A pixel was considered 'active' if its intensity was twice that of the background. A threshold of 0.15 was used to determine which regions of the islet were activate due to ChR2 stimulation compared to the islet average. The percent of the islet area that was 'active' was calculated as a proportion of the entire islet area and subsequently referred to as "Area Active". At elevated glucose, the mean Ca^{2+} time trace was averaged across the entire islet and segmented into pre and during stimulation. After detrending, a Fast Fourier Transform (FFT) was performed for both segments and the DC component subtracted. The natural oscillation frequency was identified from the pre stimulation segment as the frequency with peak power. The driving frequency was confirmed at ~0.1Hz as the frequency with peak power during stimulation.

GCaMP6 Imaging of Calcium Dynamics and Analysis: Isolated islets expressing β-cell specific GCaMP6 were incubated overnight with proinflammatory cytokines with or without S293 peptide, or S293 peptide alone. 30 Minutes prior to imaging, islets were fasted at 2 mM glucose in BMHH imaging solution. Islets were then transferred to a glass bottom dish and imaged on an LSM 800 confocal microscope. GCaMP6 fluorescence was excited at 488 nm with images collected at 1 frame/sec for approximately 80 minutes. 3-5 Minutes after the start of imaging, the glucose concentration was raised from 2 mM to 11 mM. For experiments measuring consistency between first responders and hub cells, glucose was subsequently lowered to 2 mM after achieving second phase oscillations for 10-15 minutes. After the islet had returned to basal activity without oscillations (~15 minutes), the glucose concentration was increased again to 11 mM. Samples were imaged at either x20 air or x40 water immersion and held at 37°C.

Calcium dynamics were analyzed using MATLAB. First phase response time, identification of first and last responders, and characterization of highly connected hub cells was determined as previously described [28]. Briefly, to identify the response time, we

determined the time at which individual β-cells reached their half maximum amplitude following stimulation from low to high glucose. This response time was rank ordered for all cells in the islet. The earliest 10% were classed as first responders and the latest 10% classed as last responders, as previously defined [29]. ΔT was calculated as the difference in time between the means of the last responders and first responders to capture the changes in spread between first and last responders between treatment groups relative to total time of the first phase. The percent consistency was determined as a proportion of top 10% of responding cells of the initial stimulation that were also first responders or nearest neighbors to first responders during repeated stimulation.

Highly correlated β-cell cells were identified using the calcium time-course at high glucose during the second phase. A highly correlated β-cell is a β-cell whose calcium activity strongly parallels many other β-cell in the islet. To quantify the degree of correlation, the degree of cross-correlation value obtained was obtained using the xcorr() function in MATLAB across all measured β-cell calcium time traces was compared among each cell. “Links” were derived using a threshold of correlation above 0.9. Hub cells have previously been defined as those possessing the “majority of connections” [29-30] from which we derived the criteria of >60% of functional “links” determined by mean degree of correlation above the defined threshold relative to all cells measured in the islet**.**

Statistical analysis: All statistical analysis was performed in Prism (GraphPad). A 2-sided t-test was used when comparing parameters of 2 treatment groups such as between Control versus Cytokine treated islets. Ordinary one-way ANOVA with Tukey’s *post hoc* analysis was used to compare across multiple treatment groups, where * indicates $p < 0.05$, ** indicates $p < 0.01$, *** indicates $p < 0.001$, **** indicates $p < 0.0001$. In all cases, error bars represent the standard error of the mean (S.E.M.).

220 ***Results***

221 *Successful protection of gap junction coupling by Cx36 S293 peptide under pro-inflammatory*
222 *cytokines:* To test whether functional sub-populations are disrupted by a cocktail of pro-
223 inflammatory cytokines (0.5 ng/mL IL1-β, 1 ng/mL TNF-α, and 10 ng/mL IFN-γ), and whether
224 sub-population loss depends on loss of gap junction coupling, we followed an approach
225 outlined in Figure 1A. Fluorescence Recovery After Photobleaching (FRAP) was used to
226 assess gap junction permeability and confirm a disruption to gap junction coupling by pro-
227 inflammatory cytokines (Figure 1.B) and protection of gap junction function by the Cx36 S293
228 peptide, as previously described [4]. Islets treated with pro-inflammatory cytokines showed a
229 significant reduction in gap junction permeability, as indicated by a slower recovery rate (Figure
230 1C, p=0.0300). During co-treatment with the S293 peptide, islets showed a 92.2%±38.6%
231 increase in the recovery rate compared to cytokine treatment alone. No significant difference
232 was observed between untreated control and co-treatment groups (p=0.958) or untreated
233 control vs S293 peptide alone (p=0.918). Thus, co-treatment with S293 peptide fully protects
234 gap junction permeability, consistent with previous studies that use the S293 peptide to protect
235 or recover gap junction coupling in diabetogenic environments [12].
236
237 *Protecting gap junction coupling provides a partial recovery to the cytokine-mediated disruption*
238 *of ChR2-mediated recruitment of [Ca^{2+}] at low glucose:* With the conditions established to
239 protect gap junction coupling under a diabetogenic environment, we asked whether functional
240 subpopulations of β-cells are also protected. Previous studies applied the optogenetic construct
241 ChannelRhodopsin-2 (ChR2) and single cell stimulation to discover a subpopulation of β-cells
242 with elevated metabolic activity that can recruit large numbers of neighboring cells when
243 activated at low (5 mM) glucose levels [27]. We therefore examined how pro-inflammatory
244 cytokines influenced these sub-populations and then tested the effects of preventing a decline
245 in gap junction coupling on these sub-populations.
246 Islets from $Pdx1^{PB}$-Cre;Rosa-LSL-ChR2-YFP mice that express ChR2 in β-cells were
247 loaded with the Ca^{2+} dye Rhod2. ChR2 expressing cells were subjected to focal stimulation in
248 single β-cells and the spatial Ca^{2+} response was observed in neighboring cells (Figure 2.A).
249 We quantified the proportion of β-cells in the imaging plane that showed Ca^{2+} elevations
250 coincident with ChR2 stimulation, which was repeated in ChR2-expressing islets treated with
251 the cocktail of pro-inflammatory cytokines for 1 hour (Figure 2.B) and/or Cx36 S293 peptide.

252 Under all treatments we observed heterogeneity in the recruitment of elevated [Ca^{2+}]
253 following single cell stimulation (Figure 2.C). In untreated control islets, 41.3%±4.7% of cells
254 within the imaging plane showed elevated [Ca^{2+}] following single cell stimulation, with a
255 substantial variation (Figure 2.C,D) as previously observed [27]. Treatment with pro-
256 inflammatory cytokines led to a significant decrease in the proportion of cells showing elevated
257 [Ca^{2+}] following single cell stimulation (15.4%±2.3%) compared to untreated controls (Figure
258 2.C,D, $p<0.0001$,). Co-treatment with the S293 peptide led to a moderate increase in elevated
259 [Ca^{2+}] following single cell stimulation (24.8%±2.6%), however this was still significantly lower
260 than in untreated control (Figure 2.C,D, $p=0.0026$). Treatment with S293 peptide alone showed
261 a similar proportion of cells with elevated [Ca^{2+}] (35.0%±4.5 %) to untreated control islets
262 (Figure 2.C,D, $p=0.6680$).
263 Untreated control islets showed broad heterogeneity in the recruitment of [Ca^{2+}] (Figure
264 2.C), as previously observed [27]. This included a population of cells that recruited elevated
265 [Ca^{2+}] across the islet that was above the median value in untreated control islet (>40%, Figure
266 2.C), consistent with earlier findings [27]. Under cytokine treatment (1 hour), this 'high-
267 recruiting' population of cells was almost completely absent (~4%, Figure 2.E). Co-treatment
268 with S293 peptide partially recovered this population of cells (~10%, Figure 2.E), but again less
269 than in either untreated controls or S293 peptide treatment alone. The trend in these findings
270 were similar when we applied other thresholds for the islet area recruited upon single-cell
271 stimulation (Supplemental 3.A).
272 Therefore, treatment with pro-inflammatory cytokines reduced the ChR2-mediated
273 recruitment of cells to increase [Ca^{2+}], with an abolishment of 'high-recruiting' cells. Protecting
274 gap junction coupling only partially recovers ChR2-mediatred recruitment of cells to increase
275 [Ca^{2+}], with only a small number of 'high-recruiting' cells low glucose.
276
277 *Protecting gap junction coupling recovers cytokine-mediated disruption of ChR2-mediated*
278 *recruitment of [Ca^{2+}] at high glucose:* Although protecting gap junction coupling did not
279 significantly improve single-cell mediated islet recruitment at low glucose, we sought to assess
280 whether the action of ChR2 was influenced by cytokine-mediated disruption at high glucose.
281 Islets generally respond to changes from low to high glucose by displaying a robust first phase
282 and sustained second phase within a 30-minute period. We therefore exposed islets to a high
283 glucose environment for 30 minutes during which intrinsic islet [Ca^{2+}] oscillations were

observed, confirming that the islets had entered the second phase. We then performed single-cell stimulation of ChR2-expressing β-cells as we performed at low glucose (Figure 3.A-B). In untreated control islets 62.3±1.4% of the islet within the imaging plane showed elevated [Ca^{2+}] that was coincident with the ChR2 stimulation following single cell stimulation at 0.1 Hz (Figure 3.C). This indicates how connected individual cells are across the islet. Treatment with pro-inflammatory cytokines led to a significant decrease in this [Ca^{2+}] elevation (39.7±3.4%, $p<0.01$). Co-treatment with the S293 peptide led to a full recovery in elevated [Ca^{2+}] (62.6±3.8%, $p<0.001$), indicating recovery in the overall islet connectivity.

We next investigated the extent to which islet cells were entrained, by analyzing the spectral power of the 'natural oscillation frequency' of [Ca^{2+}] oscillations that are observed prior to ChR2 stimulation and analyzing the spectral power of the [Ca^{2+}] oscillations at the frequency of the ChR2 stimulation (Figure 3.D, Supplemental 1.A). In untreated control islets the spectral power in the 'natural oscillation frequency' decreased upon single-cell ChR2 stimulation (Figure 3.E, $p<0.0001$). This was matched by an increase in the spectral power of the ChR2 driving frequency upon single-cell ChR2 stimulation (Supplemental 1.B, $p<0.0001$). Following treatment with pro-inflammatory cytokines the spectral power in the natural oscillation frequency also decreased, although this decrease was lessened compared to in control islets (Figure 3.F), indicating a less robust response to single-cell stimulation, as expected. Co-treatment with pro-inflammatory cytokines and S293 peptide increased the change in spectral power of the natural oscillation frequency compared that upon pro-inflammatory cytokines alone, and similar to that in control islets. This shows a robust recovery in the response to ChR2-mediated single-cell stimulation. Similarly, co-treatment with pro-inflammatory cytokines and S293 peptide showed a slightly increased change in spectral power at the ChR2 driving frequency, as compared to treatment with pro-inflammatory cytokines alone (Supplemental 1.C, $p = 0.2274$). These experiments were conducted over 10-20 islets per condition (from 3 ChR2-expressing mice), and our analysis indicates that treatment condition accounts for 19.9% of total variation indicating the observed differences in oscillation at high-glucose are attributed more to treatment rather than biological variability among samples.

Therefore, protecting gap junction coupling was able to fully recover islet-wide connectivity and entrainment at elevated glucose that resulted from ChR2 stimulation of individual cells.

316 *Protecting gap junction coupling does not recover the cytokine-mediated disruption to first*
317 *responder cells and the 1st phase [Ca^{2+}] response:* We next examined the impact of pro-
318 inflammatory cytokines and the protection of gap junction coupling on first responder cells and
319 the first phase [Ca^{2+}] response. Islets from Mip-Cre^{ER};ROSA26-lox-STOP-lox-GCaMP6s mice
320 that express GCaMP6 specifically in β-cells were used to assess changes in [Ca^{2+}] following
321 glucose elevation. We measured the [Ca^{2+}] response of individual cells and ranked their
322 response time after glucose stimulation. First responder cells were identified as the 10% of
323 cells which showed the earliest response, and last responders as the 10% of cells that showed
324 the latest response, with the spread in response time (Δt) being the time between first and last
325 responders (Figure 4.A). In control untreated islets the response time was consistently short
326 (Δt=179.5s$\pm$32.8s). Upon treatment with the pro-inflammatory cytokine cocktail for 1 hour, there
327 was no significant impact on the time between first and last responders (Figure 4.A-B,
328 p=0.3897). However following treatment with pro-inflammatory cytokines for 24 hours there
329 was a significant increase in the time between first and last responders compared to untreated
330 control islets (p=0.0043, Figure 4.A-B). Using this 24-hour treatment, co-treatment with S293
331 peptide did not show a decrease in Δt compared to cytokines alone (Δt=374$\pm$62s vs. 310$\pm$31s
332 respectively), indicating protection of gap junction coupling was not sufficient to recover a
333 narrow spread of the first phase response (Figure 4.C, p=0.72). Analysis of the response time
334 for first responders and last responder cells alone showed that treatment with pro-inflammatory
335 cytokines significantly increased the delay of last responding cells rather than affecting the
336 timing of first-responding cells, consistent with a reduced first-responder action (Supplemental
337 4. A,B). These findings were similar when other definitions for first-responder cells were used
338 (Supplemental 3.B). S293 peptide alone showed a similar time between first and last
339 responders as untreated controls. Under 1 hour cytokine treatment, co-treatment with the S293
340 peptide had no impact (Supplemental 2.A).
341 Clusters of first responders were previously found to be consistent upon repeated
342 glucose stimulations [28]; where ~35% of first responder cells remained first responders and
343 ~75% of first responders remained within a 1 cell distance separation. We tested whether this
344 consistency was affected by both pro-inflammatory cytokines and protection of gap junction
345 coupling. We identified the top 10% of responding cells during an initial glucose stimulation and
346 determined what proportion of these cells remained first responders or nearest neighbors to
347 first responders during a repeated glucose stimulation (Figure 4.D). Upon cytokine treatment,

348 there was a slight, but not significant, increase in the consistency of first responders upon
349 repeated glucose stimulation compared to untreated controls (57.9% vs. 38% respectively, p =
350 0.2835, Figure 4.E). Upon protection of gap junction coupling via co-treatment with S293
351 peptide there was a slight, but not significant, decrease in the consistency of first responders
352 relative to cytokine only treatment (39.5%, p = 0.3264, Figure 4.E), and similar to that measured
353 in untreated controls. The consistency of first responders after 1 hour of cytokine treatment
354 also did not significantly improve upon co-treatment with the S293 peptide (Supplemental 2.B).
355 Therefore, treatment with pro-inflammatory cytokines disrupted the first-phase timing,
356 which was impacted by the protection of gap junction coupling. However pro-inflammatory
357 cytokines increased the consistency of the first phase [Ca^{2+}] response, which was reversed
358 upon protection of gap junction coupling.
359
360 *Protection of gap junction coupling provides a partial recovery to the cytokine-mediated*
361 *disruption of of highly connected β-cell hubs:* Finally, we examined the impact of pro-
362 inflammatory cytokines and the protection of gap junction coupling on highly connected β-cell
363 hubs. β-cell hubs have been demonstrated to maintain coordinated [Ca^{2+}] dynamics [25,28,29],
364 and previous work indicated a decrease in β-cell hubs upon diabetogenic conditions [13,29].
365 Following Ca^{2+} imaging we analyzed individual cell time-courses and formed a functional
366 network and identified the most highly connected cells as β-cell hubs (Figure 5.A, see
367 Methods). In control islets the number of highly synchronized functional connections and highly
368 synchronized hubs was high and consistent with prior measurements [29,30]. Upon treatment
369 with pro-inflammatory cytokines for 1 hour, there was no significant impact the mean degree of
370 correlation (Figure 5.B, p=0.3708). However following treatment with pro-inflammatory
371 cytokines for 24 hours, there was a significant decrease in the mean degree of correlation
372 (Figure 5.B, p=0.008 and Figure 5.C, p = 0.0375). There was also a significant decrease in
373 proportion of highly synchronized functional connections or “links” (Figure 5.D, p=0.0094) and
374 modest decrease in highly connected β-cell hubs (Figure 5.E, p=0.3759). Co-treatment with
375 S293 peptide did not show a significant change in neither functional connection nor β-cell hubs
376 compared to cytokines alone (Figure 5.C-E, p=0.9832 and p=0.8101 respectively). While the
377 proportion of hub-like cells across the entire β-cell population slightly increased upon co-
378 treatment with the S293 peptide compared to cytokine-treated islets, this was not statistically
379 significant. This indicates that protection of gap junction coupling was not sufficient to recover
380 highly synchronized functional connections and highly connected β-cell hubs. S293 peptide

381 alone showed similar functional connections and β-cell hubs as untreated controls. These
382 findings were similar when other definitions for highly-connected cells were used
383 (Supplemental 3.C). Under 1 hour cytokine treatment, co-treatment with S293 had no impact
384 on mean correlation or number of links per islet (Supplemental 2.C,D).

385 Approximately 43% of β-cell hubs remained as hubs following repeated glucose
386 stimulation under control conditions (Figure 5.F). We tested whether this consistency is affected
387 by both pro-inflammatory cytokines and protection of gap junction coupling. Upon cytokine
388 treatment, there was a decrease in the consistency of hubs (31%) compared to untreated
389 control islets. Protection of gap junction coupling via co-treatment with S293 peptide showed a
390 trend toward improved consistency of hubs compared to cytokine treatment alone (66%,
391 p=0.2109, Figure 5.G), with similar measurements to S293 peptide treatment alone, albeit
392 lacking statistical significance. Under 1 hour cytokine treatment, co-treatment with S293 did not
393 increase the population of hub cells as a percent, per islet (Supplement 2.E,F).

394 Therefore, treatment with pro-inflammatory cytokines reduced the presence of highly
395 synchronized functional connections and β-cell hubs. Restoration of gap junction coupling, and
396 subsequent islet-wide synchronization has little influence on hubs but maintains the
397 consistency of those remaining hub cells.

398

399 ***Discussion***

400 Cx36 gap junctions have previously been identified as important regulators of β-cell
401 coordination and islet function through the electrical coupling of neighboring β-cells.
402 Pharmacological or genetic improvements in Cx36 gap junctions has been shown to recover
403 [Ca^{2+}] and insulin secretion responses in models of diabetes *in vitro*, and delay onset of
404 diabetes *in vivo*, indicating a protective role that gap junctions play in islet function [12,31].
405 Functional sub-populations, which emerge as a result of β-cell heterogeneity, have been
406 identified, and these sub-populations can drive the coordinated islet electrical response [27].
407 The goal of this study was to examine the influence of gap junctions on functional sub-
408 populations of β-cells in a cytokine-mediated diabetogenic environment. Towards this, in the
409 presence of a cocktail of pro-inflammatory cytokines, we protected Cx36 gap junction coupling
410 using a peptide which we previously developed [12]. We then applied both optogenetics and
411 calcium imaging to measure cell recruitment and calcium dynamics to identify and characterize
412 three functional sub-populations that have previously been described [28] including first
413 responders and hubs. Gap junction coupling could be successfully protected under pro-
414 inflammatory conditions, and this was accompanied by recovery in islet-wide entrainment by
415 ChR2 stimulation. However, optogenetic stimulation, and/or analysis of calcium dynamics
416 revealed that functional subpopulations remained largely impaired. We conclude that while
417 Cx36 gap junction coupling is critical for overall islet coordination and emergence of functional
418 sup-populations, protection of gap junctions is not sufficient to recover the loss of these
419 subpopulations upon cytokine-mediated disruption. Therefore cell-intrinsic properties are likely
420 more influential in driving the impairment of functional sub-populations under diabetogenic
421 conditions.

422

423 <u>*Impairment of functional sub-populations under diabetogenic conditions:*</u> Increased levels of
424 proinflammatory cytokines within the islet microenvironment, including IL1-β and TNF-α, is a
425 key feature of diabetes and has been attributed to driving islet dysfunction [16,32,33]. Prior
426 studies have found that functional sub-populations are also disrupted in diabetes, such as
427 reduced numbers of β-cell hubs under both pro-inflammatory cytokines and glucolipotoxic
428 conditions [29], reduced consistency of wave initiator/leader cells under high-fat diet conditions
429 [15] and reduced presence of hubs and leaders in islets from human subjects with type2
430 diabetes [34]. In this study we extended these findings to show both the cells that recruit a large
431 proportion of the neighbors to show elevated [Ca^{2+}] upon stimulation at low glucose ('high-

432 recruiting'), and the response time of first responder cells that respond earliest to glucose were
433 both disrupted by pro-inflammatory cytokines. This points to a general occurrence for functional
434 sub-populations to be disrupted under diabetogenic conditions. Notably, each of these
435 functional sub-population is associated with driving a specific aspect of islet electrical response,
436 which were also disrupted under the pro-inflammatory cytokines. For example, β-cell hubs
437 coordinate oscillatory dynamics across the islet, and the synchronization of these oscillations
438 was disrupted by pro-inflammatory cytokines. First responders coordinate and enhance the
439 initial first-phase response to glucose elevation, which was also disrupted by pro-inflammatory
440 cytokines. Thus, disruption to these functional sub-populations may be contributing to islet
441 dysfunction under diabetogenic conditions.
442
443 *Influence of gap junction disruption to functional subpopulations under diabetogenic conditions*:
444 Functional sub-populations, such as β-cell hubs, first-responders, and those that show high
445 ChR2-recruitment of [Ca^{2+}] at low glucose, all exert their influence to coordinate and recruit
446 other β-cells via Cx36 gap junction coupling. Therefore, we hypothesized that pro-inflammatory
447 cytokines disrupt these sub-populations and their action because of diminished gap junction
448 coupling. By using the S293 peptide we could recover functional gap junction coupling
449 equivalent to that in control untreated islets indicated by FRAP. However, we did not observe
450 substantial recoveries in the presence and action of functional sub-populations when gap
451 junctions were protected: we observed only partial recovery to ChR2-recruitment at low
452 glucose, a slight recovery of β-cell hubs and no recovery to first responders. One simple
453 explanation is non-specific effects of the S293 peptide, however prior studies did not observe
454 non-specific effects on [Ca^{2+}]. Further, we observed a recovery in islet-wide entrainment of
455 [Ca^{2+}] dynamics upon ChR2 stimulation at elevated glucose, which is expected to be more
456 dependent on gap junction electrical coupling and thus confirms the effects of the S293 peptide.
457 These findings therefore indicate that the disruptions to functional sub-populations under pro-
458 inflammatory cytokines are not primarily due to disruptions to gap junction coupling.
459 While initially unexpected, our findings are consistent with the fact that gap junction
460 coupling is not per se a defining feature of these sub-populations. For example, cells with high
461 ChR2-recruitment at low glucose do not show increased gap junction coupling [27], β-cell hubs
462 do not show increased gap junction coupling [30], and first responders show lower gap junction
463 coupling [28]. Thus, gap junction coupling does not drive the formation of these sub-
464 populations, rather they are defined by cell-intrinsic properties such as elevated glucose

465 metabolism or electrical differences, as well as other environmental properties such as the
466 potential influence of α- or δ-cells [35]. Dysfunction to these cell intrinsic properties or altered
467 communication with α- or δ-cells is therefore likely driving their disruption. However, as
468 discussed above, we note that some amount of gap junction coupling will still be required for
469 these cells to exert their influence across the islet [3].

470 Enhancing gap junction coupling can recover islet function in diabetogenic conditions
471 [12,16,36]. Indeed, we observed a recovery in overall islet entrainment at elevated glucose by
472 ChR2 stimulation. This enhanced function has also been demonstrated via both genetic and
473 pharmacological approaches in models of diabetes *in vitro* and *in vivo*. While promising, our
474 findings indicate that targeting gap junction coupling alone will be insufficient to fully recover
475 islet function, given that functional β-cell sub-populations will still be disrupted. For example,
476 caloric restriction is able to improve islet dysfunction that results from a high-fat diet; yet, while
477 gap junction coupling recovered, wave initiators/leaders did not [15]. Inclusion of the GLP1R
478 agonist Exendin-4 with pro-inflammatory cytokines recovered gap junction coupling and
479 coordinated [Ca^{2+}] dynamics [37], while also impacting insulin secretion pathways via cAMP
480 signaling. Thus, ensuring intrinsic factors and/or communication with α- and δ-cells are
481 recovered will likely be required. Future work should examine which of these factors is
482 important to both define functional sub-populations and preserve their action on islet function
483 under diabetogenic conditions.

484

485 *Limitations and Future Work:* Our findings indicate that protection of gap junctions alone is not
486 sufficient to recover cytokine-mediated loss of functional subpopulations. However, other
487 factors within the islet microenvironment during diabetes can also impact islet function,
488 including gluco- and lipotoxicity, amyloid plaque formation, and other pro-inflammatory
489 cytokines such as IL6. Thus, extending our findings to other invitro treatments and mouse
490 models of diabetes will be needed in future work. Another important factor is that our study
491 examined a 24-hour treatment with pro-inflammatory cytokines and/or S293 peptide. This
492 compares to a 1-6 hour treatment time in previous studies that support the recovery of gap
493 junctions and islet function by S293 [12]. While we observed a protection of gap junction
494 coupling, it is possible that under more acute treatments we will observe some recovery in
495 functional sub-populations and a further enhancement in gap junction coupling, given that Cx36
496 turnover has a half-life of ~3 hours [38]. After 24 hours of cytokine treatment, observed loss of
497 functional subpopulations may therefore result from effects of prolonged cytokine exposure in

addition to disrupted gap junctions, further supporting our conclusion that recovery of gap junctions alone is not sufficient in restoring functional subpopulations under diabetogenic conditions. Nevertheless, a longer-term treatment is likely more reflective of the islet microenvironment in diabetes and should be further studied. Lastly, we acknowledge that our study primarily focuses on β-cells despite potential influences of other existing cell types including α- and δ-cells on β-cell behavior. Further studies addressing intercellular crosstalk is necessary to fully understand the global effects of cytokine treatment and the role of gap junctions.

Summary: Overall, we demonstrate that proinflammatory cytokines disrupt the presence and action of functional β-cell sub-populations such as hubs and first responders, as well as the cell-recruitment of [Ca^{2+}]. Preventing the decline in gap junction coupling was not sufficient for recovering these functional β-cell sub-populations. This correlates with gap junction coupling not being a factor that defines β-cell heterogeneity within the islet, but rather cell intrinsic properties or other aspects of intra-islet communication instead being disrupted by the pro-inflammatory environment.

515 ***Figure Descriptions***

516 **Figure 1.** Restoration of cytokine-mediated disruptions to gap junction coupling, as measured
517 by Fluorescence Recovery After Photobleaching (FRAP). (A) Isolated mouse islets were
518 treated with a cocktail of pro-inflammatory cytokines (0.5 ng/mL IL1-β, 1 ng/mL TNF-α, and 10
519 ng/mL IFN-γ) and co-incubated with 30 μM S293 peptide for 1 hour before imaging. (B)
520 Representative image of Rhodamine123 loaded islet pre- and post-photobleaching, along with
521 FRAP time-course after photobleaching, showing fluorescence recovery in the bleached
522 region. (C) Rate of recovery was calculated as a proxy for gap junction permeability in
523 untreated, cytokine, cytokine plus S293 peptide, and S293 peptide alone treatments. Data
524 represents Mean ± S.E.M. with each islet represented by a data point (from 6 mice), and each
525 measurement is normalized to the mean control value per mouse. * indicates $p < 0.05$.
526

527 **Figure 2***.* Impact of gap junction restoration on the cytokine-mediated disruption to ChR2-
528 mediated recruitment of [Ca^{2+}]. (A) A ChR2-expressing islet (left), where a single ChR2-YFP
529 expressing cell was stimulated at 0.1 Hz (i) and calcium response was recorded across the
530 islet which exhibited both regions of recruited (ii) and unrecruited (iii) cells in untreated
531 conditions (middle). The result [Ca^{2+}] activity was then quantified (right). (B) As in A, under
532 cytokine-treated conditions. (C) Histogram indicating the proportion of the islet recruited by a
533 single cell stimulation under each treatment condition. (D) Mean proportion of the islet recruited
534 by a single cell stimulation under each treatment condition. Data represents Mean ± S.E.M.
535 with each islet represented by a data point (from 15 mice). (E) The proportion of cells that were
536 able to recruit an area larger than 40% of the islet under the cytokine and S293 conditions
537 indicated. ** indicates $p < 0.01$, **** indicates $p < 0.0001$.
538

539 **Figure 3.** Impact of gap junction restoration *on* ChR2 single cell stimulation and islet
540 entrainment at high glucose. (A) Representative calcium responses, where a single ChR2-YFP
541 expressing cell was stimulated at 0.1 Hz at elevated glucose (i), and calcium response was
542 recorded across the islet which exhibited both regions of recruited/entrained (ii) and
543 unrecruited/not entrained (iii) cells. The result [Ca^{2+}] activity was then quantified (right). (B) As
544 in A, under cytokine-treated conditions. (C) Mean proportion of the islet recruited by a single
545 cell at high glucose. Data presented as Mean ± S.E.M. with each islet. (D) Power spectra of
546 the [Ca^{2+}] oscillation in control islets pre-ChR2 stimulation (top) and during-stimulation

547 (bottom). The dominant natural oscillation frequency (NOF) is highlighted in blue and the ChR2
548 driving frequency is highlighted in orange (E). Mean normalized power of the NOF, pre and
549 post ChR2 stimulation under each treatment condition. (F) Ratio of the spectral power of the
550 NOF pre/post stimulation. Data represents Mean ± S.E.M. with each experimental islet
551 represented by a data point. All data represents n = 3 mice, 2-3 islets per condition per mouse.
552 * indicates $p < 0.05$, ** indicates $p < 0.01$, *** indicates $p < 0.001$, **** indicates $p < 0.0001$.
553
554 **Figure 4.** Impact of gap junction restoration on the cytokine-mediated disruption to the temporal
555 and spatial consistency of first responders. (A) Time-course of [Ca^{2+}] in first responder cells
556 (red) and last responder cells (green) following stimulation by high (11mM) glucose, under
557 control or cytokine-treated conditions (for 1h or 24h). (B) The mean time spread between the
558 first and last responders (ΔT) in islets treated with cytokines for 24 hours or 1 hour, compared
559 to untreated. Data represents Mean ± S.E.M. with each islet represented by a data point (n =
560 4 mice). (C) The mean time spread in islets treated for 24 hours, with cytokines and/or S293
561 peptide recovery of gap junction coupling. (D) Time-course of [Ca^{2+}] in first responder cells
562 (red) and last responder cells (green), subjected to repeated stimulation from low to high
563 glucose (E) The percent consistency of first responders in untreated cells (~40%) or those with
564 cytokines and/or S293 peptide recovery of gap junction coupling. Data represents Mean ±
565 S.E.M. with each islet represented by a data point (n = 9 mice). ** indicates $p < 0.01$, ***
566 indicates $p < 0.001$.
567
568 **Figure 5.** Impact of gap junction restoration on the cytokine-mediated disruption of highly
569 connected β-cell hubs. (A) Representative connectivity map (above) and time-courses (below)
570 of islets under control or cytokine-treated conditions (for 1h or 24h). (B) The mean correlation
571 coefficient in islets treated with cytokines for 24 hours or 1 hour, compared to untreated. (C)
572 Mean correlation coefficient in islets treated for 24 hours, with cytokines and/or S293 peptide
573 recovery of gap junction coupling. (D) As in C for the average number of links between cells.
574 (E) As in C for the proportion of hub cells among the entire islet cell population. (F) Time-course
575 of [Ca^{2+}] in β-cell hubs that are consistent or not consistent, together with representative
576 connectivity maps. (G) The percent consistency of hubs in untreated cells (>50%) or those with
577 cytokines and/or S293 peptide recovery of gap junction coupling. Data represents Mean ±

578 S.E.M. with each islet represented by a data point (n = 10 mice). * indicates $p < 0.05$, **
579 indicates $p < 0.01$, *** indicates $p < 0.001$.
580
581 **Supplement 1.** Spectral analysis of ChR2 single cell stimulation at high glucose. (A) Power
582 spectra of the [Ca^{2+}] oscillation in control islets post-ChR2 stimulation. The natural oscillation
583 frequency (NOF) is highlighted in blue and the ChR2 driving frequency is highlighted in orange
584 (B). Mean normalized power of the ChR2 driving frequency, pre and post ChR2 stimulation
585 under each treatment condition. Data presented as Mean ± S.E.M. with each experimental islet
586 represented by a data point. (C) Ratio of the spectral power of the ChR2 driving frequency
587 post/pre stimulation averaged across all islets. Data presented as Mean ± S.E.M. with each
588 experimental islet represented by a data point. All data represents n = 3 mice, 2-3 islets per
589 condition per mouse. * indicates $p < 0.05$, ** indicates $p < 0.01$, *** indicates $p < 0.001$, ****
590 indicates $p < 0.0001$.
591
592 **Supplement 2.** First responder and hub cells under 1h cytokine treatment with/without gap
593 junction restoration. (A) The mean time spread in islets treated for 1 hour, with cytokines and/or
594 S293 peptide recovery of gap junction coupling. (B) The percent consistency of first responders
595 in untreated cells (~40%) or those with cytokines and/or S293 peptide recovery of gap junction
596 coupling. (C) Mean correlation coefficient in islets treated for 1 hour, with cytokines and/or S293
597 peptide recovery of gap junction coupling. (D) As in C for the average number of links between
598 cells. (E) As in C for the proportion of hub cells among the entire islet cell population. (F) As in
599 C for percent consistency of hubs. Data represents Mean ± S.E.M. with each islet represented
600 by a data point (n = 4 mice).
601
602 **Supplement 3.** Threshold-dependent variation in defined subpopulations. (A) The proportion
603 of cells that were able to recruit an area larger than 30%, 40% and 50% of the islet upon single
604 cell ChR2-stimulation. Data represents mean area across all islets per condition. (B) The mean
605 time spread between the first and last responders (ΔT) defined as the earliest and latest 10%
606 of cells, earliest and latest 20% of cells and earliest 5 cells and latest 5 cells. (C) Population of
607 hub cells per islet and corresponding highest number of links for correlation thresholds of 0.9,
608 0.8, and 0.5. Data represents Mean ± S.E.M. with each islet represented by a data point (n =
609 4 mice).

610 **Supplement 4.** Time of first and last responder cells after 24h cytokine treatment with/without
611 gap junction restoration. (A) The exact time of the 10% of fastest responding β-cells to reach
612 first phase after stimulation with high glucose (B) The exact time of the 10% of slowest
613 responding β-cells to reach first phase after stimulation with high glucose. Data represents
614 Mean ± S.E.M. with each cell represented by a data point (n = 9 mice) ** indicates $p < 0.01$, ***
615 indicates $p < 0.001$, **** indicates $p < 0.0001$.

616 ***References***

617 1. Federation, I.D. *Diabetes around the world in 2021*. 2022 [cited 2024.
618 2. Allagnat, F., D. Martin, D.F. Condorelli, G. Waeber, and J.-A. Haefliger, *Glucose represses*
619 *connexin36 in insulin-secreting cells.* Journal of cell science, 2005. **118**(22): p. 5335-5344.
620 3. Benninger, R.K., M. Zhang, W.S. Head, L.S. Satin, and D.W. Piston, *Gap junction coupling and*
621 *calcium waves in the pancreatic islet.* Biophysical journal, 2008. **95**(11): p. 5048-5061.
622 4. Farnsworth, N.L., A. Hemmati, M. Pozzoli, and R.K. Benninger, *Fluorescence recovery after*
623 *photobleaching reveals regulation and distribution of connexin36 gap junction coupling within*
624 *mouse islets of Langerhans.* The Journal of physiology, 2014. **592**(20): p. 4431-4446.
625 5. Ravier, M.A., M. Guldenagel, A. Charollais, A. Gjinovci, D. Caille, G. Sohl, C.B. Wollheim, K.
626 Willecke, J.-C. Henquin, and P. Meda, *Loss of connexin36 channels alters β-cell coupling, islet*
627 *synchronization of glucose-induced Ca2+ and insulin oscillations, and basal insulin release.*
628 Diabetes, 2005. **54**(6): p. 1798-1807.
629 6. Pipeleers, D.G., *Heterogeneity in pancreatic β-cell population.* Diabetes, 1992. **41**(7): p. 777-
630 781.
631 7. Stožer, A., M. Gosak, J. Dolenšek, M. Perc, M. Marhl, M.S. Rupnik, and D. Korošak, *Functional*
632 *connectivity in islets of Langerhans from mouse pancreas tissue slices.* PLoS computational
633 biology, 2013. **9**(2): p. e1002923.
634 8. Benninger, R.K., W.S. Head, M. Zhang, L.S. Satin, and D.W. Piston, *Gap junctions and other*
635 *mechanisms of cell–cell communication regulate basal insulin secretion in the pancreatic islet.*
636 The Journal of physiology, 2011. **589**(22): p. 5453-5466.
637 9. Speier, S., A. Gjinovci, A. Charollais, P. Meda, and M. Rupnik, *Cx36-mediated coupling reduces*
638 *β-cell heterogeneity, confines the stimulating glucose concentration range, and affects insulin*
639 *release kinetics.* Diabetes, 2007. **56**(4): p. 1078-1086.
640 10. Head, W.S., M.L. Orseth, C.S. Nunemaker, L.S. Satin, D.W. Piston, and R.K. Benninger, *Connexin-*
641 *36 gap junctions regulate in vivo first-and second-phase insulin secretion dynamics and glucose*
642 *tolerance in the conscious mouse.* Diabetes, 2012. **61**(7): p. 1700-1707.
643 11. Hodson, D.J., R.K. Mitchell, E.A. Bellomo, G. Sun, L. Vinet, P. Meda, D. Li, W.-H. Li, M. Bugliani,
644 and P. Marchetti, *Lipotoxicity disrupts incretin-regulated human β cell connectivity.* The Journal
645 of clinical investigation, 2013. **123**(10): p. 4182-4194.
646 12. St. Clair, J.R., M.J. Westacott, J. Miranda, N.L. Farnsworth, V. Kravets, W.E. Schleicher, J.M.
647 Dwulet, C.H. Levitt, A. Heintz, and N.W. Ludin, *Restoring connexin-36 function in diabetogenic*
648 *environments precludes mouse and human islet dysfunction.* The Journal of Physiology, 2023.
649 **601**(18): p. 4053-4072.
650 13. Farnsworth, N.L., R.L. Walter, A. Hemmati, M.J. Westacott, and R.K. Benninger, *Low level pro-*
651 *inflammatory cytokines decrease connexin36 gap junction coupling in mouse and human islets*
652 *through nitric oxide-mediated protein kinase Cδ.* Journal of Biological Chemistry, 2016. **291**(7):
653 p. 3184-3196.
654 14. Carvalho, C.d.F., R.B. Oliveira, A. Britan, J. Santos-Silva, A.C. Boschero, P. Meda, and C.B.
655 Collares-Buzato, *Impaired β-cell-β-cell coupling mediated by Cx36 gap junctions in prediabetic*
656 *mice.* American Journal of Physiology-Endocrinology and Metabolism, 2012. **303**(1): p. E144-
657 E151.
658 15. Corezola do Amaral, M.E., V. Kravets, J.M. Dwulet, N.L. Farnsworth, R. Piscopio, W.E.
659 Schleicher, J.G. Miranda, and R.K. Benninger, *Caloric restriction recovers impaired β-cell-β-cell*
660 *gap junction coupling, calcium oscillation coordination, and insulin secretion in prediabetic*

mice. American Journal of Physiology-Endocrinology and Metabolism, 2020. **319**(4): p. E709-E720.

16. Farnsworth, N.L., R.A. Piscopio, and R.K. Benninger, *Modulation of gap junction coupling within the islet of langerhans during the development of type 1 diabetes.* Frontiers in Physiology, 2022. **13**: p. 913611.
17. Westacott, M.J., N.L. Farnsworth, J.R. St. Clair, G. Poffenberger, A. Heintz, N.W. Ludin, N.J. Hart, A.C. Powers, and R.K. Benninger, *Age-dependent decline in the coordinated [Ca2+] and insulin secretory dynamics in human pancreatic islets.* Diabetes, 2017. **66**(9): p. 2436-2445.
18. Ravier, M., J. Sehlin, and J. Henquin, *Disorganization of cytoplasmic Ca 2+ oscillations and pulsatile insulin secretion in islets from ob/ob mice.* Diabetologia, 2002. **45**: p. 1154-1163.
19. Heimberg, H., A. De Vos, A. Vandercammen, E. Van Schaftingen, D. Pipeleers, and F. Schuit, *Heterogeneity in glucose sensitivity among pancreatic beta-cells is correlated to differences in glucose phosphorylation rather than glucose transport.* The EMBO journal, 1993. **12**(7): p. 2873-2879.
20. Roscioni, S.S., A. Migliorini, M. Gegg, and H. Lickert, *Impact of islet architecture on β-cell heterogeneity, plasticity and function.* Nature Reviews Endocrinology, 2016. **12**(12): p. 695-709.
21. Wang, Y.J., J. Schug, K.-J. Won, C. Liu, A. Naji, D. Avrahami, M.L. Golson, and K.H. Kaestner, *Single-cell transcriptomics of the human endocrine pancreas.* Diabetes, 2016. **65**(10): p. 3028-3038.
22. Wojtusciszyn, A., M. Armanet, P. Morel, T. Berney, and D. Bosco, *Insulin secretion from human beta cells is heterogeneous and dependent on cell-to-cell contacts.* Diabetologia, 2008. **51**: p. 1843-1852.
23. Benninger, R.K., T. Hutchens, W.S. Head, M.J. McCaughey, M. Zhang, S.J. Le Marchand, L.S. Satin, and D.W. Piston, *Intrinsic islet heterogeneity and gap junction coupling determine spatiotemporal Ca2+ wave dynamics.* Biophysical journal, 2014. **107**(11): p. 2723-2733.
24. Giordano, E., D. Bosco, V. Cirulli, and P. Meda, *Repeated glucose stimulation reveals distinct and lasting secretion patterns of individual rat pancreatic B cells.* The Journal of clinical investigation, 1991. **87**(6): p. 2178-2185.
25. Benninger, R.K. and V. Kravets, *The physiological role of β-cell heterogeneity in pancreatic islet function.* Nature Reviews Endocrinology, 2022. **18**(1): p. 9-22.
26. Rutter, G.A., A. Gresch, L. Delgadillo Silva, and R.K. Benninger, *Exploring pancreatic beta-cell subgroups and their connectivity.* Nature metabolism, 2024: p. 1-15.
27. Westacott, M.J., N.W. Ludin, and R.K. Benninger, *Spatially organized β-cell subpopulations control electrical dynamics across islets of Langerhans.* Biophysical journal, 2017. **113**(5): p. 1093-1108.
28. Kravets, V., J.M. Dwulet, W.E. Schleicher, D.J. Hodson, A.M. Davis, L. Pyle, R.A. Piscopio, M. Sticco-Ivins, and R.K. Benninger, *Functional architecture of pancreatic islets identifies a population of first responder cells that drive the first-phase calcium response.* PLoS Biology, 2022. **20**(9): p. e3001761.
29. Johnston, N.R., R.K. Mitchell, E. Haythorne, M.P. Pessoa, F. Semplici, J. Ferrer, L. Piemonti, P. Marchetti, M. Bugliani, and D. Bosco, *Beta cell hubs dictate pancreatic islet responses to glucose.* Cell metabolism, 2016. **24**(3): p. 389-401.
30. Briggs, J.K., A. Gresch, I. Marinelli, J.M. Dwulet, D.J. Albers, V. Kravets, and R.K. Benninger, *β-cell intrinsic dynamics rather than gap junction structure dictates subpopulations in the islet functional network.* Elife, 2023. **12**: p. e83147.

31. Farnsworth, N.L., R.A. Piscopio, W.E. Schleicher, D.G. Ramirez, J.G. Miranda, and R.K. Benninger, *Modulation of gap junction coupling within the islet of langerhans during the development of type 1 diabetes.* Frontiers in Physiology, 2022. **13**: p. 913611.
32. Akash, M.S.H., K. Rehman, and S. Chen, *Role of inflammatory mechanisms in pathogenesis of type 2 diabetes mellitus.* Journal of cellular biochemistry, 2013. **114**(3): p. 525-531.
33. Alexandraki, K., C. Piperi, C. Kalofoutis, J. Singh, A. Alaveras, and A. Kalofoutis, *Inflammatory process in type 2 diabetes: The role of cytokines.* Annals of the New York Academy of Sciences, 2006. **1084**(1): p. 89-117.
34. Gosak, M., R. Yan-Do, H. Lin, P.E. MacDonald, and A. Stožer, *Ca2+ oscillations, waves, and networks in islets from human donors with and without type 2 diabetes.* Diabetes, 2022. **71**(12): p. 2584-2596.
35. Jin, E., J.K. Briggs, R.K. Benninger, and M.J. Merrins, *Glucokinase activity controls subpopulations of β-cells that alternately lead islet Ca2+ oscillations.* bioRxiv, 2024.
36. Klee, P., F. Allagnat, H. Pontes, M. Cederroth, A. Charollais, D. Caille, A. Britan, J.-A. Haefliger, and P. Meda, *Connexins protect mouse pancreatic β cells against apoptosis.* The Journal of clinical investigation, 2011. **121**(12): p. 4870-4879.
37. Farnsworth, N.L., R. Walter, R.A. Piscopio, W.E. Schleicher, and R.K. Benninger, *Exendin-4 overcomes cytokine-induced decreases in gap junction coupling via protein kinase A and Epac2 in mouse and human islets.* The Journal of physiology, 2019. **597**(2): p. 431-447.
38. Wang, H.Y., Y.-P. Lin, C.K. Mitchell, S. Ram, and J. O'Brien, *Two-color fluorescent analysis of connexin 36 turnover: relationship to functional plasticity.* Journal of cell science, 2015. **128**(21): p. 3888-3897.

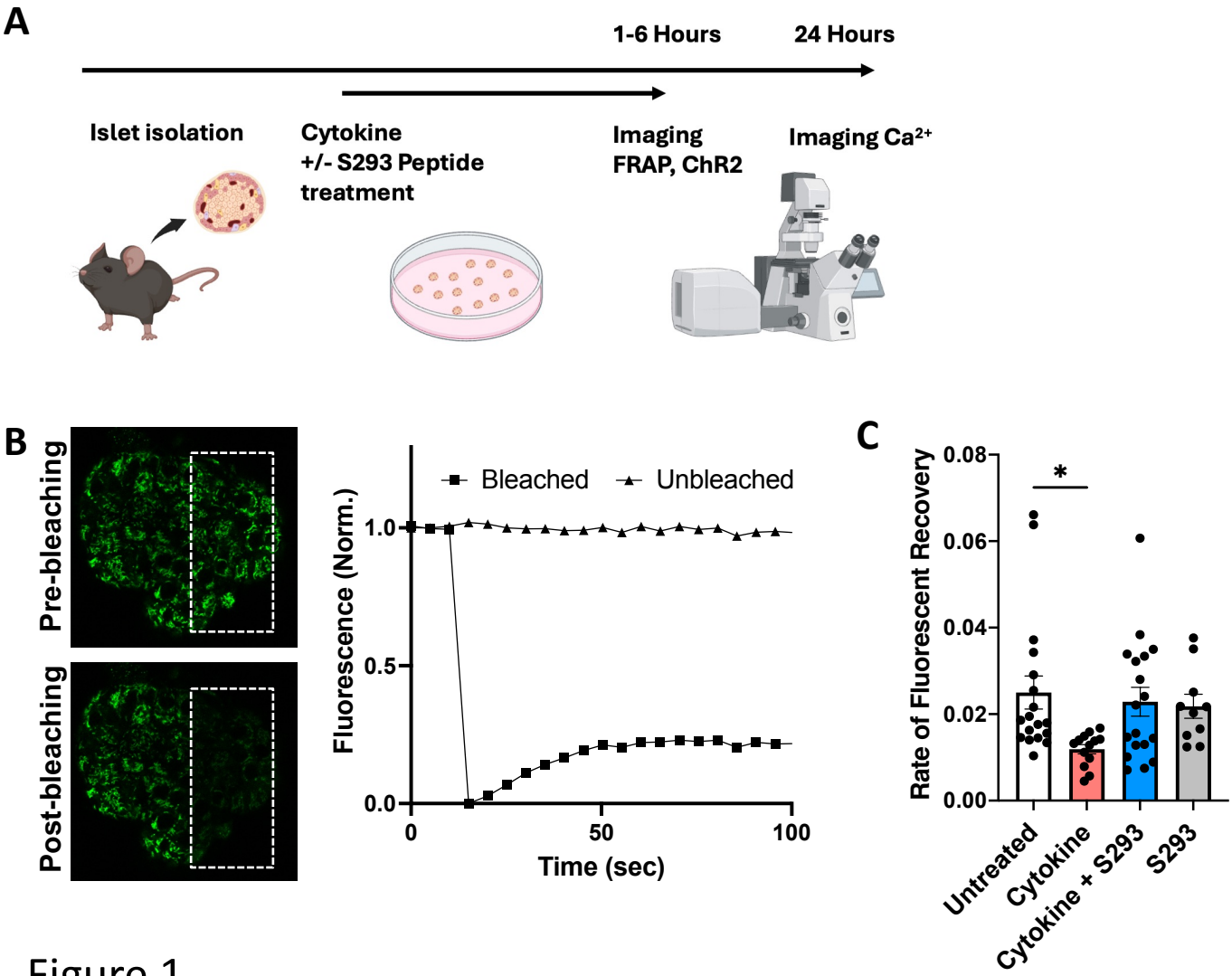
A
1-6 Hours
24 Hours
Islet isolation
Cytokine
+/- S293 Peptide
treatment
Imaging
FRAP, ChR2
Imaging Ca2+
B
Pre-bleaching
Post-bleaching
Bleached
Unbleached
Fluorescence (Norm.)
1.0
0.5
0.0
0
50
100
Time (sec)
C
Rate of Fluorescent Recovery
0.08
0.06
0.04
0.02
0.00
*
Untreated
Cytokine
Cytokine + S293
S293

Figure 1

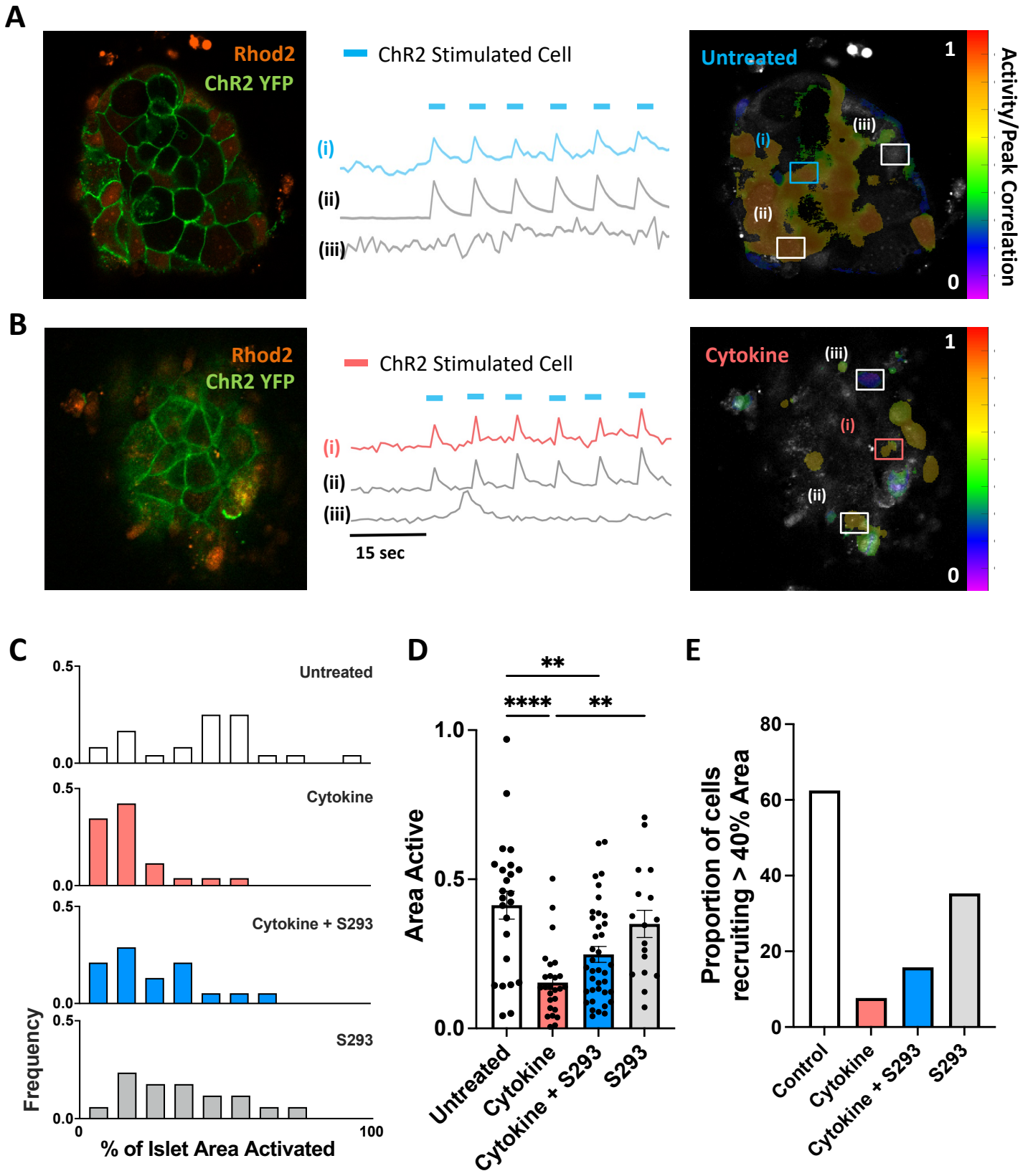
A
Rhod2
ChR2 YFP
ChR2 Stimulated Cell
(i)
(ii)
(iii)
Untreated
1
0
Activity/Peak Correlation
B
Rhod2
ChR2 YFP
ChR2 Stimulated Cell
(i)
(ii)
(iii)
15 sec
Cytokine
1
0
C
Untreated
Cytokine
Cytokine + S293
S293
0.5
0.0
Frequency
0
100
% of Islet Area Activated
D
**
****
**
Area Active
1.0
0.5
0.0
Untreated
Cytokine
Cytokine + S293
S293
E
Proportion of cells recruiting > 40% Area
80
60
40
20
0
Control
Cytokine
Cytokine + S293
S293

Figure 2

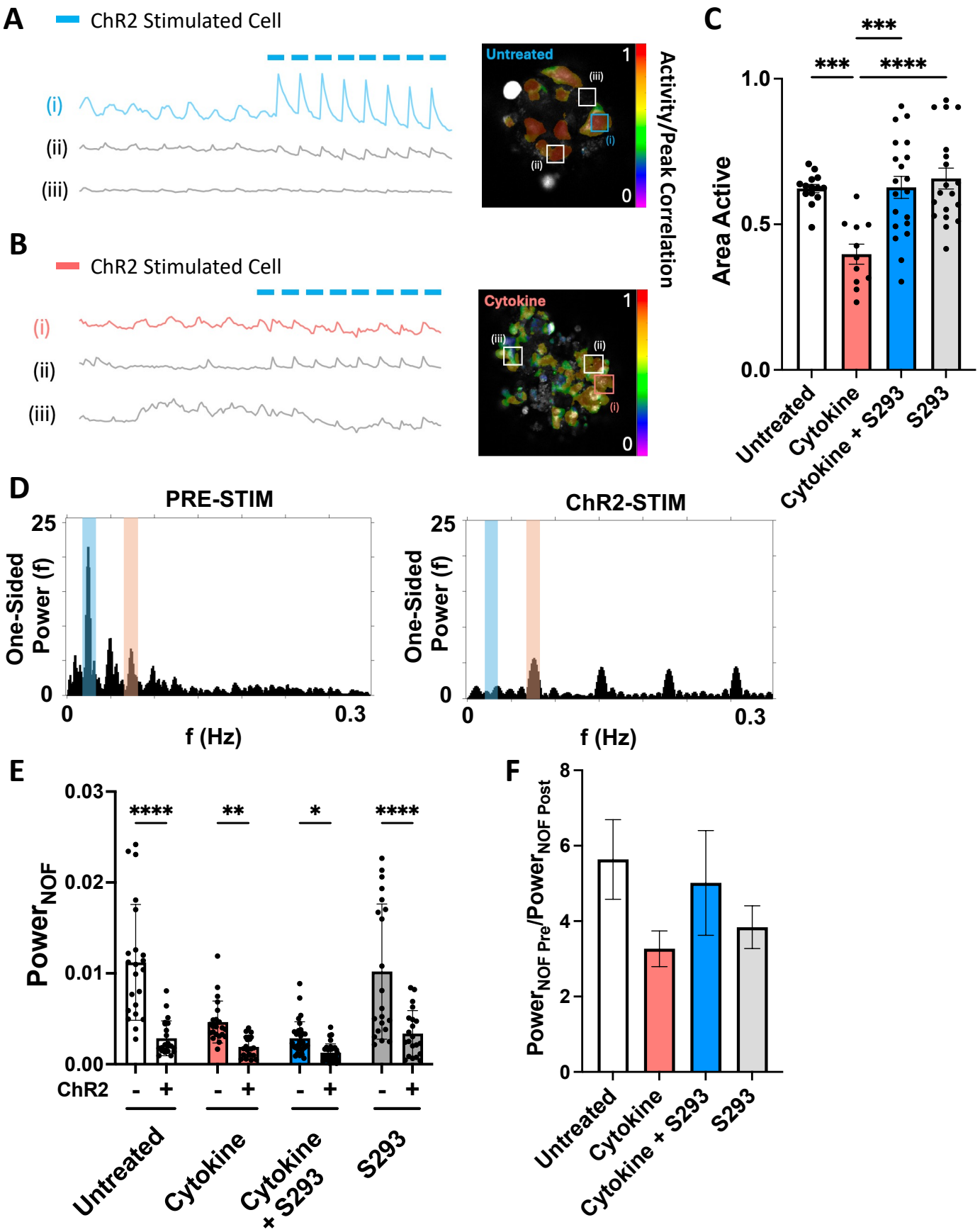
A
ChR2 Stimulated Cell
(i)
(ii)
(iii)
Untreated
1
0
Activity/Peak Correlation
B
ChR2 Stimulated Cell
Cytokine
C
Area Active
1.0
0.5
0.0
***
****
Untreated
Cytokine
Cytokine + S293
S293
D
PRE-STIM
ChR2-STIM
One-Sided Power (f)
25
0
0.3
f (Hz)
E
Power$_{NOF}$
0.03
0.02
0.01
0.00
****
**
*
ChR2
-
+
Untreated
Cytokine
Cytokine + S293
S293
F
Power$_{NOF\ Pre}$/Power$_{NOF\ Post}$
8
6
4
2
0

Figure 3

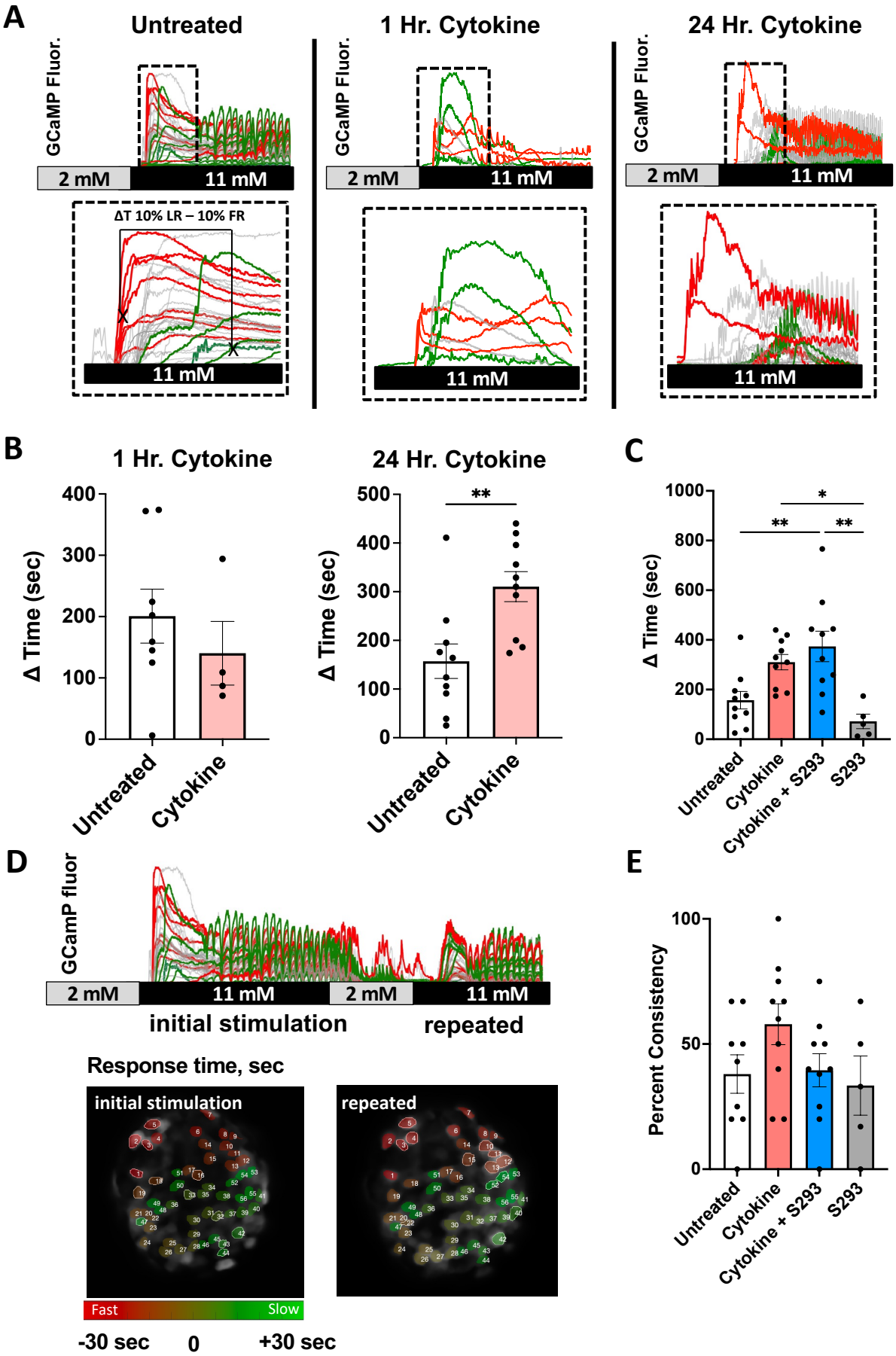
A
Untreated
1 Hr. Cytokine
24 Hr. Cytokine
GCaMP Fluor.
2 mM
11 mM
ΔT 10% LR – 10% FR
B
1 Hr. Cytokine
24 Hr. Cytokine
Δ Time (sec)
Untreated
Cytokine
C
Cytokine + S293
S293
D
GCamP fluor
initial stimulation
repeated
Response time, sec
Fast
Slow
-30 sec
0
+30 sec
E
Percent Consistency

Figure 4

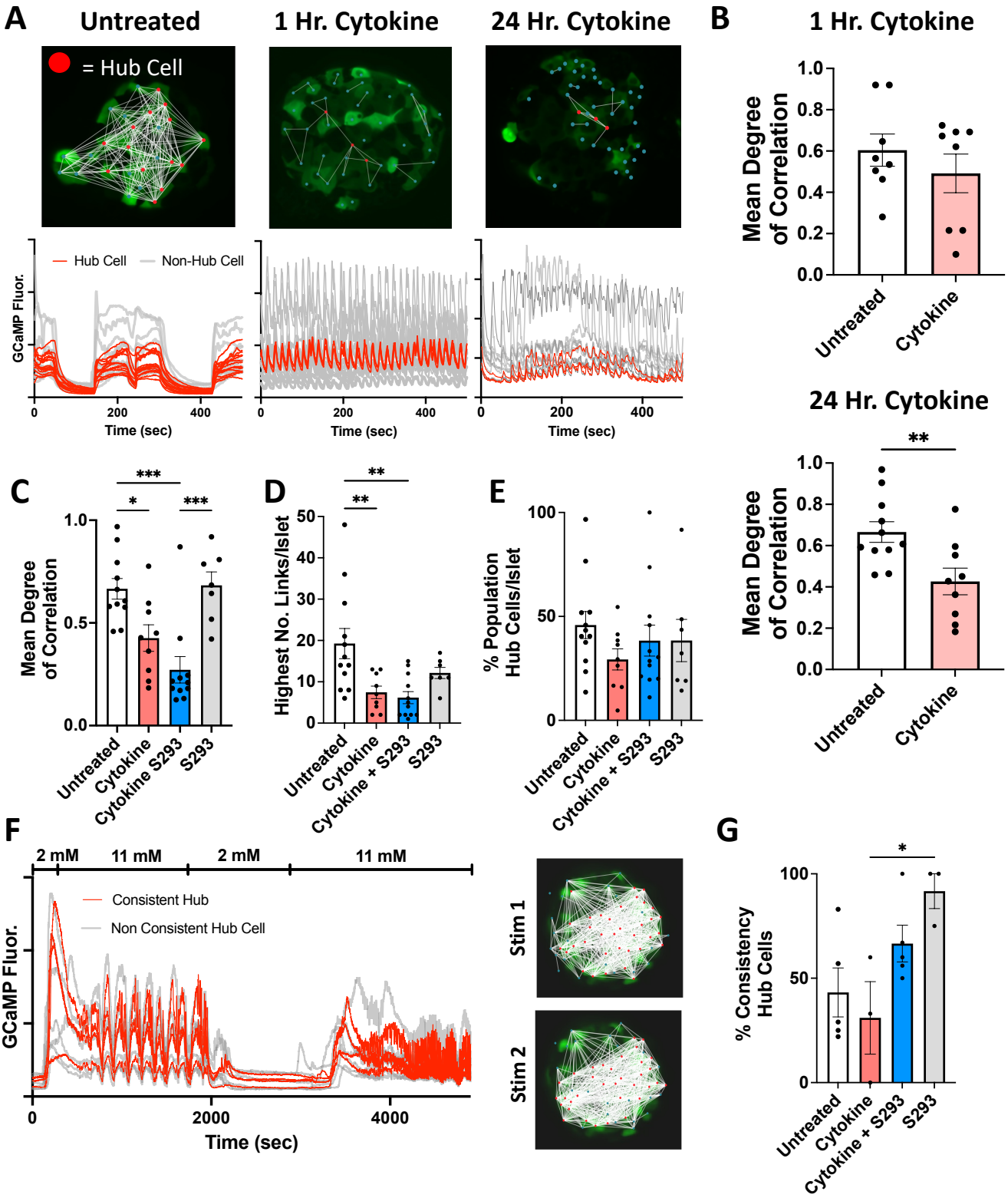
A
Untreated
1 Hr. Cytokine
24 Hr. Cytokine
= Hub Cell
Hub Cell
Non-Hub Cell
GCaMP Fluor.
Time (sec)
B
1 Hr. Cytokine
Mean Degree of Correlation
Untreated
Cytokine
24 Hr. Cytokine
C
Mean Degree of Correlation
Untreated
Cytokine
Cytokine S293
S293
D
Highest No. Links/Islet
Cytokine + S293
E
% Population Hub Cells/Islet
F
2 mM
11 mM
Consistent Hub
Non Consistent Hub Cell
Stim 1
Stim 2
G
% Consistency Hub Cells

Figure 5

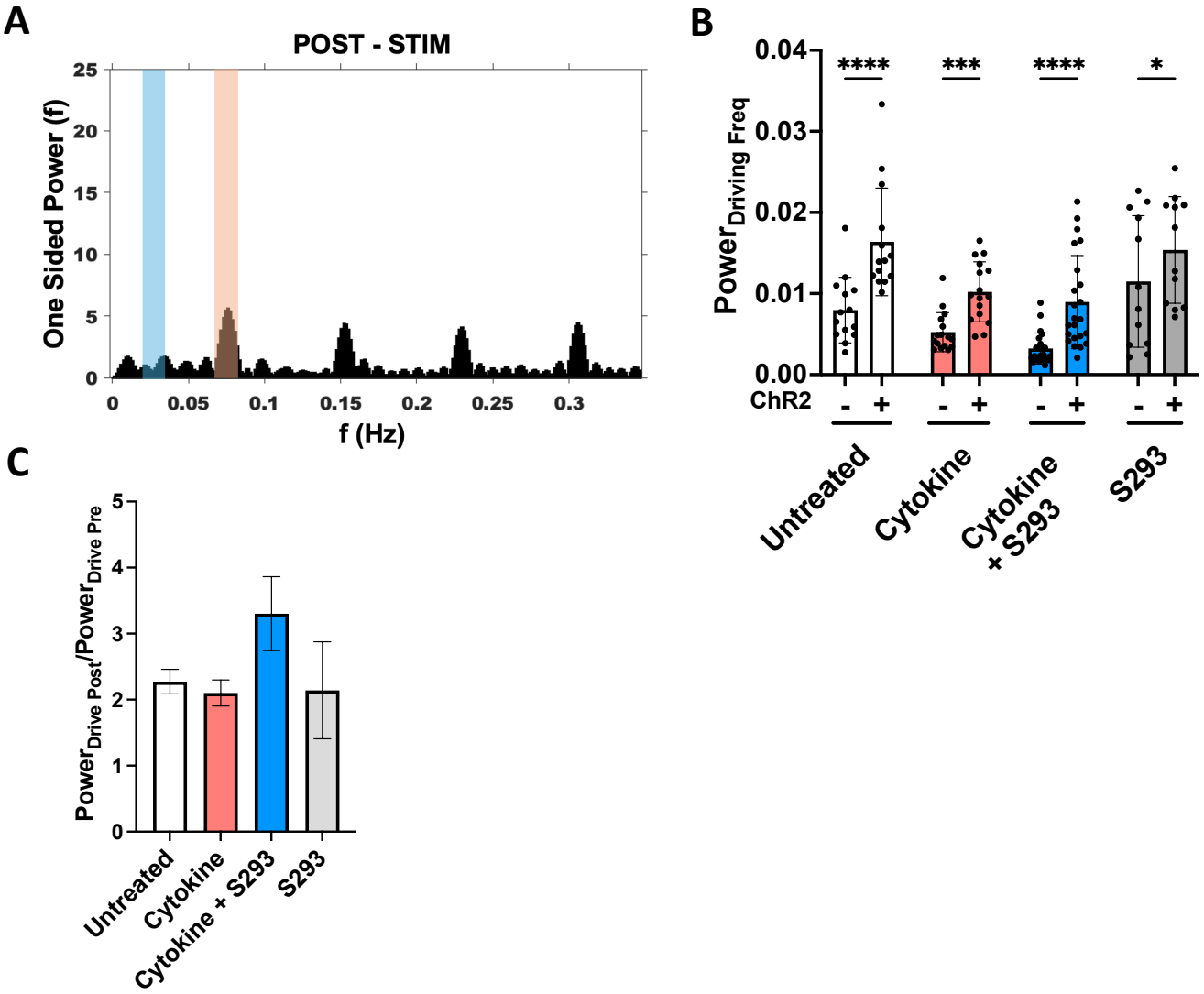

Supplemental Figure S1

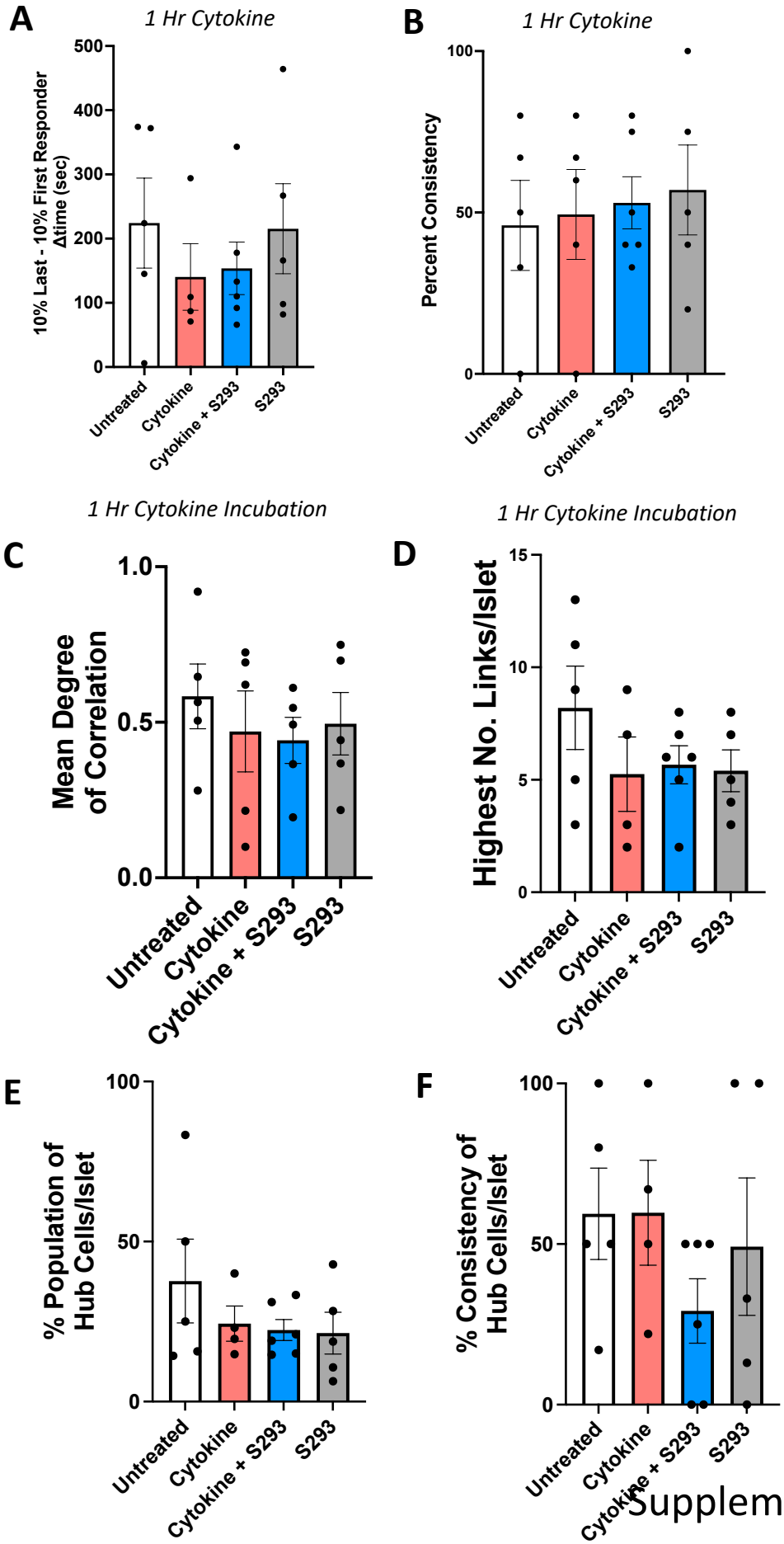

Supplemental Figure S2

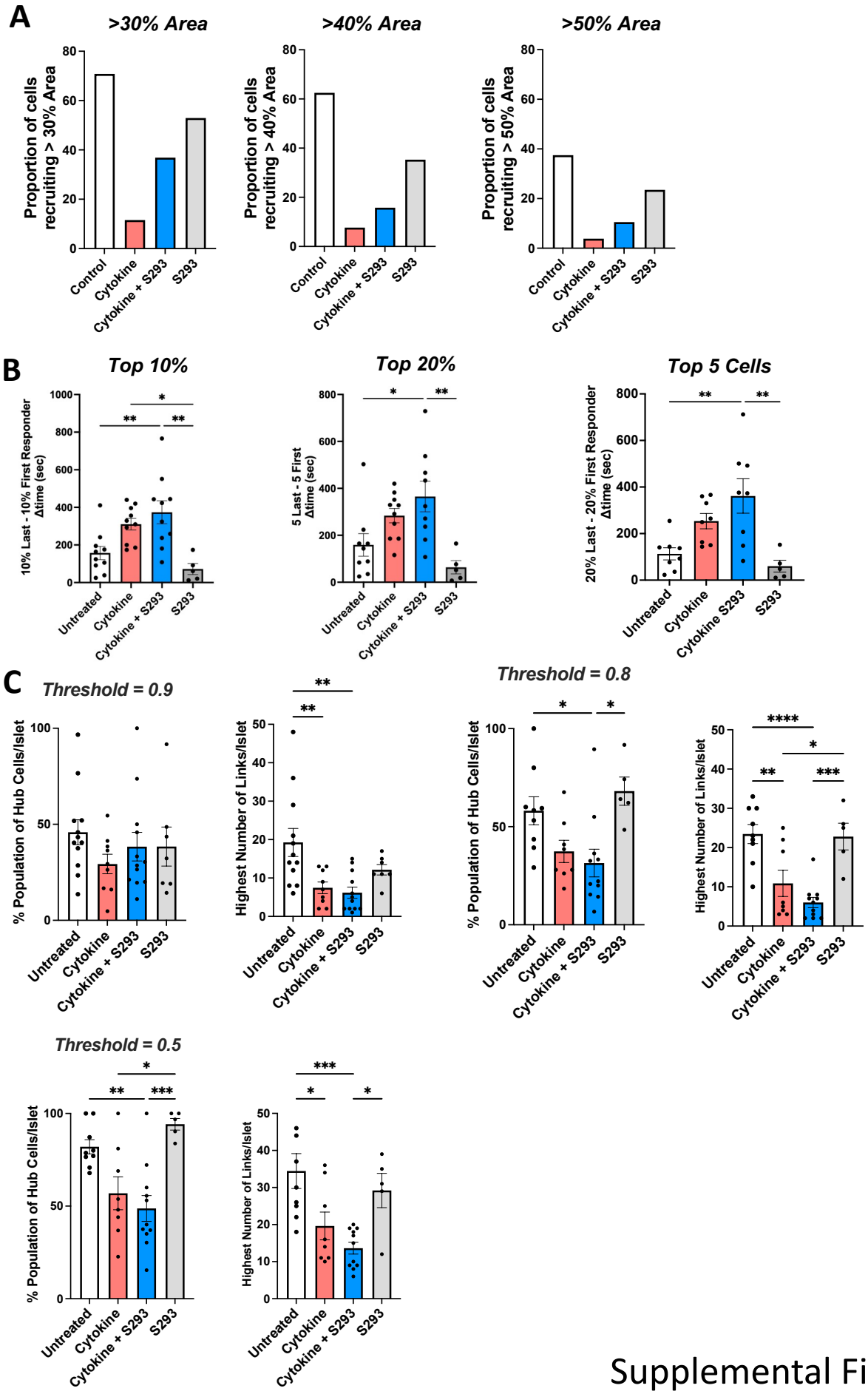

Supplemental Figure S3

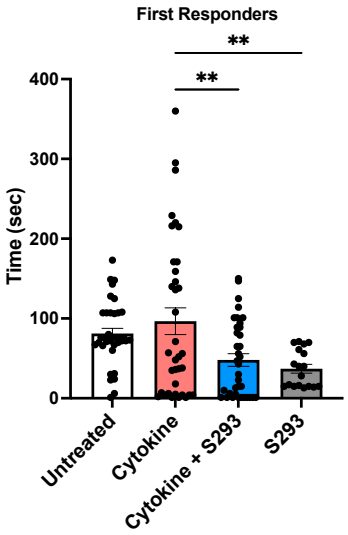

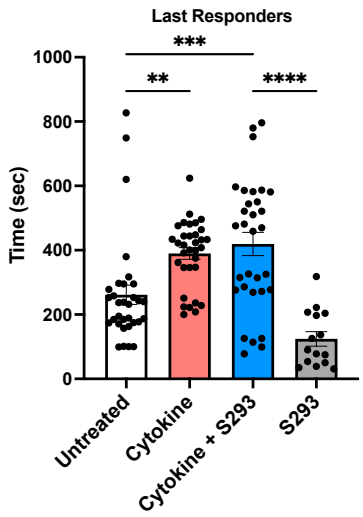

Supplemental Figure S4